Local order in liquids forming quasicrystals and approximant phases

V. Simonet,[1] F. Hippert,[2] M. Audier,[2] and R. Bellissent[3,*]
[1]*Laboratoire de Physique des Solides (UA CNRS 02), Université de Paris-Sud, 91405 Orsay Cedex, France*
[2]*Laboratoire des Matériaux et du Génie Physique (UMR CNRS 5628), ENSPG, BP46, 38402 Saint Martin d'Hères, France*
[3]*Laboratoire Leon Brillouin (CEA-CNRS), CE Saclay, 91191 Gif sur Yvette, France*
(Received 30 July 2001; published 19 December 2001)

Neutron-scattering experiments were performed on liquid $Al_{88.5}(Mn_xCr_{1-x})_{11.5}$ alloys ($0 \leqslant x \leqslant 1$), giving rise to equilibria with μ phase compounds whose structure is closely related to those of quasicrystalline phases. Assuming a Mn/Cr isomorphic substitution like the one existing in the μ phase, partial pair structure factors and corresponding correlation functions were determined in these liquids. The results show a strong (Mn-Cr)-Al chemical order where the average first coordination shell around transition-metal atoms appears to be in agreement with an icosahedral local order. Simulations based on liquid models containing icosahedral clusters like those existing in many Al-Mn-Cr intermetallic structures are found to reproduce the liquid total structure factors measured at large momentum transfer where the influence of local order is preponderant. Information on icosahedral local order is also obtained when such a simulation method is applied to other liquid alloys, $Al_{92.3}Mn_{7.7}$, $Al_{81}Pd_{19}$, and $Al_{72.1}Pd_{20.7}Mn_{7.2}$, giving rise to approximant or quasicrystalline phases, but in which partial functions are not determined.

DOI: 10.1103/PhysRevB.65.024203 PACS number(s): 61.20.−p, 61.12.−q, 61.25.Mv

I. INTRODUCTION

It is generally assumed that phenomena such as amorphous state formation, undercooling effects, or the solidification of metastable and stable phases of primary crystallization depend on the nature of the local order in liquid phases. For instance, if a high solid-liquid interfacial energy (or a high activation threshold for nucleation) must be invoked in the case of deeply undercooled metallic melts, the reason for this could be the existence in undercooled melts of energetically favorable clusters whose structure is not compatible with the translational invariance of crystals (see, for instance, the recent review article by Holland-Moritz[1]). The idea that structures of undercooled liquid metals could be based on packings of icosahedral units constituted of 13 atoms was first suggested by Franck.[2] The reasons given by this author were twofold: (i) A periodic crystal with the symmetry of a regular icosahedron is excluded as the icosahedral point group is noncrystallographic. (ii) Assuming a Lennard-Jones potential for atomic interactions, an icosahedral cluster of 13 atoms has a lower energy per atom than that of a close-packed cluster of 13 atoms compatible with either fcc or hcp crystalline structures. Although any experimental result on the local order of undercooled bulk metallic melt has not been obtained so far,[1] a development of an icosahedral local order increasing with the undercooling temperature depth of the melt was found by molecular dynamics simulations on Lennard-Jones liquids.[3,4]

However, with the discovery by Shechtman *et al.*[5] of quasiperiodic structures with icosahedral symmetry, new questions have arisen about the relationship between short-range order in liquid alloys and long-range icosahedral order in this state of matter. In particular, one can ask whether a liquid and a quasicrystalline solid exhibit similar local orders when they are in equilibrium, and what the relation with undercooling effects is in this case. Let us recall that several authors[6,7] first attempted to describe a quasicrystalline state by icosahedral glass models, because the first samples prepared by Shechtman *et al.*[5] were obtained as metastable phases by melt spinning liquid Al-Mn and Al-Cr alloys. In these models, it was assumed that liquids forming quasicrystals exhibit a strong icosahedral local order well above their melting point. These models were progressively abandoned when stable quasicrystalline phases, exhibiting diffraction reflections as narrow as those of periodic crystals of very good quality, were found in different ternary alloys (e.g., Al-Fe-Cu, Al-Pd-Mn, and Mg-Zn-Y). Nevertheless, it seems still reasonable to assume an icosahedral local order in the corresponding equilibrium liquid phases, as the long-range order in quasicrystals might precisely be a consequence of such a local order.

Indeed, the results of neutron-scattering studies by Maret and co-workers on liquid $Al_{80}Mn_{20}$ (Refs. 8 and 9) and $Al_{71}Pd_{19}Mn_{10}$ (Ref. 10) alloys, with compositions close to those of icosahedral phases, were interpreted by molecular-dynamics simulations[11] as being characteristic of the presence of icosahedral local order in liquid alloys above their melting point. We also carried out neutron scattering studies on liquid Al-Pd-Mn alloys with Mn contents between 3.5 and 7.2 at.%.[12,13] But, at variance with the samples studied by Maret and co-workers,[8–10] the sample compositions were chosen such that the liquid can reach a thermodynamical equilibrium upon cooling with the icosahedral quasicrystal or an approximant phase presenting icosahedral local order.[14] The presence of a strong icosahedral local order in the liquid state could be suggested from the overall similarity observed between the structure factors of liquids and equilibrium solid phases, and on the basis of theoretical predictions of Sachdev and Nelson.[15,16] This conclusion was also upheld by simulations of the structure factor at large momentum transfers (Q) using a liquid model of icosahedral clusters. In addition, from these neutron-scattering measurements at low momentum transfer combined with susceptibility measurements and additional polarized neutron-scattering experiments, it was

established that magnetic moments appear on melting on Mn atoms which are nonmagnetic in the solid,[12,13] the paramagnetism continuing to increase with temperature in the liquid state. The origin of this behavior was discussed in relation to an evolution of the local icosahedral order in the liquid when the temperature increases.[13] However, simulations at large momentum transfers are not sufficient to ascertain what type of local order occurs in ternary alloys. A determination of the partial distribution functions is necessary for a better characterization of the local order in these liquid alloys, and of its link with magnetism.

Although partial distribution functions were already determined in liquid Al-Mn-(Fe-Cr) and Al-Pd-Mn-(Fe-Cr) alloys,[8–10] assuming that a substitution of Mn atoms by a (Fe-Cr) atomic mixture is isomorphic, we have obtained evidences[17–19] that it could be more readily achieved and ascertained in liquid $Al_{88.5}(Mn_xCr_{1-x})_{11.5}$ alloys. In a previous work, we showed that a liquid-$\mu Al_{80.5}(Mn_yCr_{1-y})_{19.5}$ phase equilibrium exists with a complete Mn/Cr substitution range in the μ structure. These liquids can be considered as ideal for neutron-scattering studies for several reasons. (i) The Mn/Cr substitution in the μ structure is isomorphic,[17,19] which therefore yields a convincing argument for inferring that an isomorphic substitution occurs as well in the equilibrium liquid phase. (ii) Important neutron-scattering contrast effects are expected, allowing an accurate determination of partial distribution functions, as the neutron scattering lengths of Cr and Mn are very different (of opposite sign).[20] (iii) The chemical composition of both μAl_4Mn and μAl_4Cr compounds correspond to those of metastable icosahedral phases.[21] (iv) The μ phase is an approximant structure of icosahedral phases and exhibits an icosahedral local order around its transition metal atoms.[22] (v) The magnetic properties of $Al_{88.5}Mn_{11.5}$ and $Al_{88.5}Cr_{11.5}$ liquid alloys, probed by susceptibility measurements,[23] are very similar to those of Al-Pd-Mn liquids.[13]

We have therefore performed neutron-scattering experiments on a set of $Al_{88.5}(Mn_xCr_{1-x})_{11.5}$ liquids with $x=1$, 0.745, 0.494, 0.246, and 0. Experimental results are presented in Sec. II. A preliminary report on these results can be found in Ref. 24. Partial distribution functions are determined using the formalism of Faber and Ziman[25] and Bhatia and Thornton[26] (Sec. III). An analysis of the total structure factor based on a local icosahedral order in the liquid state is also proposed from simulations at large momentum transfers (Sec. IV). An excellent agreement is found between these two analyses which allows one to establish the existence of an icosahedral local order in $Al_{88.5}(Mn_xCr_{1-x})_{11.5}$ liquids, and which validates the use of a simulation of the structure factor at large Q to probe the local order. We then apply such simulations to several other liquids, in equilibrium with approximant and quasicrystalline phases, for which partial functions were not determined. We study a liquid $Al_{92.3}Mn_{7.7}$ whose stoechiometry could accommodate Al icosahedral clusters centered on Mn atoms. The primary crystallization of this liquid is the $\mu Al_{80.5}Mn_{19.5}$ phase. Another interesting feature of this alloy is that its Mn content is close to that of $Al_{72.1}Pd_{20.7}Mn_{7.2}$ liquid, previously studied[13] and used for the growth of large icosahedral single crystals. In order to clarify the role of Pd atoms in this latter alloy, we also studied a $Al_{81}Pd_{19}$ liquid alloy. The product of primary crystallization of the $Al_{81}Pd_{19}$ liquid is the orthorhombic phase o-Al_3Pd,[27] almost isomorphous to the approximant ξ'-AlPdMn phase.[28] Experimental results on these liquids are presented in Sec. II and simulations of their structure factor at large Q in Sec. IV.

TABLE I. Compositions of the liquid alloy samples. The liquidus temperature (T_L) observed by differential thermal analysis and the temperature of measurement are indicated for each liquid alloy, respectively.

Liquid alloys	T_L (K)	T measure (K)
$Al_{88.5}(Mn_1Cr_0)_{11.5}$	1169	1343
$Al_{88.42}(Mn_{0.745}Cr_{0.255})_{11.58}$	1253	1343
$Al_{88.5}(Mn_{0.494}Cr_{0.506})_{11.5}$	1278	1343
$Al_{88.56}(Mn_{0.246}Cr_{0.754})_{11.44}$	1288	1343
$Al_{88.49}(Mn_0Cr_1)_{11.51}$	1295	1343
$Al_{92.3}Mn_{7.7}$	1140	1223
$Al_{81}Pd_{19}$	1050	1173
$Al_{72.1}Pd_{20.7}Mn_{7.2}$	1160	1223

II. EXPERIMENTS

A. Samples

$Al_{88.5}(Mn_xCr_{1-x})_{11.5}$ samples were the same as those prepared for the purpose of the metallurgical study on the Al-Cr-Mn system[18] where the elements of purity Al 99.999 wt %, Mn 99.9 wt %, and Cr 99.99 wt % were made molten in a cold crucible induction furnace under an argon atmosphere. Experiments on liquid alloys were carried out on five samples whose compositions and liquidus temperatures T_L are indicated in Table I. According to the results of Ref. 18, obtained on thermodynamic liquid-solid equilibria in the Al-rich corner of the Al-Mn-Cr system, all these sample compositions belong to a liquidus phase field in equilibrium with an $\mu Al_{80.5}(Mn_yCr_{1-y})_{19.5}$ phase (with $0 \leqslant y \leqslant 1$). Such equilibria are recalled in Fig. 1, where the alloy sample compositions are reported. From a differential thermal analysis, the temperatures T_L, corresponding to the beginning of a primary crystallization of μ phase compounds from the liquid, vary from 1169 to 1295 K as x decreases from 1 to 0 (Table I). The binary $Al_{92.3}Mn_{7.7}$ and $Al_{81}Pd_{19}$ alloys were prepared by induction melting from pure elements.

B. Neutron-scattering measurements

Neutron-scattering experiments on $Al_{88.5}(Mn_xCr_{1-x})_{11.5}$ liquids at 1343 K were performed on the spectrometer D4B of the high flux reactor at ILL (Grenoble), using a wavelength λ of 0.7026 Å. The scattered intensities were measured through two 64-cell moving detectors in a Q range of 0.2–14 $Å^{-1}$. The $Al_{92.3}Mn_{7.7}$ and $Al_{81}Pd_{19}$ samples were measured at 1173 and 1223 K, respectively, using the spectrometer 7C2 of the Orphée reactor at LLB (Saclay), where a fixed 640-cell detector allowed to record neutron scattering in a Q range from 0.5 to 16 $Å^{-1}$, with a value of λ of 0.705

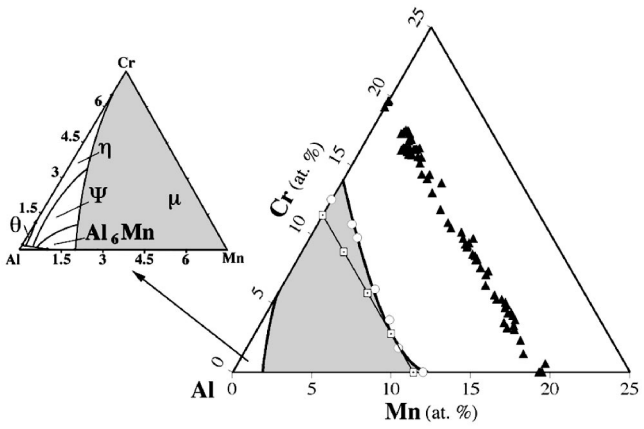

FIG. 1. Projection of an Al-Mn-Cr liquidus phase field (in gray) in equilibrium with μ phase compounds (from Ref. 18), where triangular points represent the μ phase compositions obtained from solidification of liquid samples of initial compositions represented as empty disks. The compositions of the five liquid alloy samples used in the present study are represented by square points. The enlarged part of the projection shows liquidus phase fields corresponding to the solidification of other solid phases.

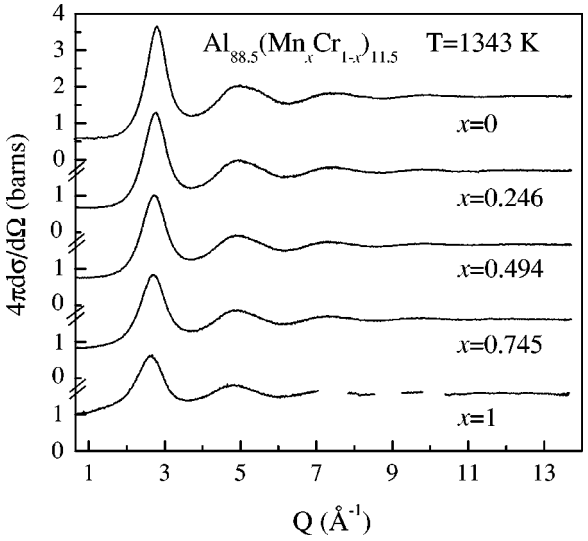

FIG. 2. Differential scattering cross section of the five $Al_{88.5}(Mn_xCr_{1-x})_{11.5}$ liquids.

Å. Each sample, heated in a tungsten (D4B) or vanadium (7C2) resistor furnace, was molten in a single-crystal sapphire container which does not react with these liquid alloys. The orientation of each container around the vertical axis (perpendicular to the scattering plane) was set in order to avoid Bragg reflections. However, because of the low-Q resolution of the spectrometers used (± 0.1 Å^{-1} for D4B and ± 0.2 Å^{-1} for 7C2), Bragg tails could not be completely eliminated. The scattering of the empty container was then measured at temperatures corresponding to those of the experiment before introducing the sample. The sample (cylindrical ingots) masses were about 15 g.

C. Data analysis

At a given temperature the differential scattering cross section of the sample $(d\sigma/d\Omega)(Q)$ was obtained by subtracting, from the spectrum of the full container, the spectrum of the empty sapphire container within the furnace multiplied by a temperature-independent proportionality coefficient α, and the spectrum of the empty furnace multiplied by $1-\alpha$. For each sample the α value was adjusted so that any trace of the sapphire scattering could not be detected in the final spectra. The α values were found to vary between 0.91 and 0.93 for the different samples. They are in agreement with the transmission factor calculated following the method of Paalman and Pings,[29] provided that both scattering and absorption processes are taken into account. The low value of both the absorption and scattering cross sections ensures that the transmission coefficient is almost independent of the scattering angle. A Plazeck correction for inelastic scattering[30,31] and a standard multiple-scattering correction[32] were carried out. A vanadium sample with a geometry identical to that of the samples was measured in order to obtain an absolute normalization of the cross sections. In all cases, the asymptotic value of $4\pi(d\sigma/d\Omega)(Q)$ at large Q coincides, within a few percent, with the calculated total scattering cross section $\sigma_T=\sigma_i+4\pi\langle b^2\rangle$, where $\sigma_i=\Sigma_j c_j\sigma_{inc}^j$ and $\langle b^2\rangle=\Sigma_j c_j\overline{b_j^2}$ [σ_{inc} is the intrinsic incoherent scattering cross section (isotopic and nuclear spin mixture contributions), $\overline{b_j}$ the average scattering length, and c_j the concentration of the jth element (Al, Mn, Cr, or Pd) (Ref. 20)]. Such an agreement validated the corrections applied to the measured neutron scattered intensities. In the following we have normalized the data so that the asymptotic value of the differential scattering cross section at large Q is equal to σ_T. The experimental structure factor $S_{expt}(Q)$ is related to the differential scattering cross section by

$$S_{expt}(Q)=[4\pi d\sigma/d\Omega(Q) - \sigma_i - 4\pi d\sigma_{mag}/d\Omega(Q)]/4\pi\langle b^2\rangle, \quad (1)$$

with $d\sigma_{mag}/d\Omega(Q)$ the paramagnetic contribution.

D. Results

Differential scattering cross sections measured on liquid $Al_{88.5}(Mn_xCr_{1-x})_{11.5}$ alloys at 1343 K are shown in Fig. 2. Slight moves of the sapphire container during the heating process produced Bragg contaminations of the $Al_{88.5}Mn_{11.5}$ liquid spectrum in several Q ranges for Q larger than 7 Å^{-1}. These data have been removed.

The amplitude of the oscillations of liquid spectra increases, and their maxima are shifted toward larger Q values, as x decreases. Hereafter we shall show that this evolution is due to the difference between Mn and Cr scattering lengths, the structure of the liquid remaining the same whatever the value of x. The differential scattering cross section measured at small-Q values contains paramagnetic contributions that appear in the liquid state, and increase as a function of the Mn/Cr ratio.

In Fig. 3(a), the differential scattering cross section of liquid $Al_{92.3}Mn_{7.7}$ and $Al_{81}Pd_{19}$ alloys are compared to that

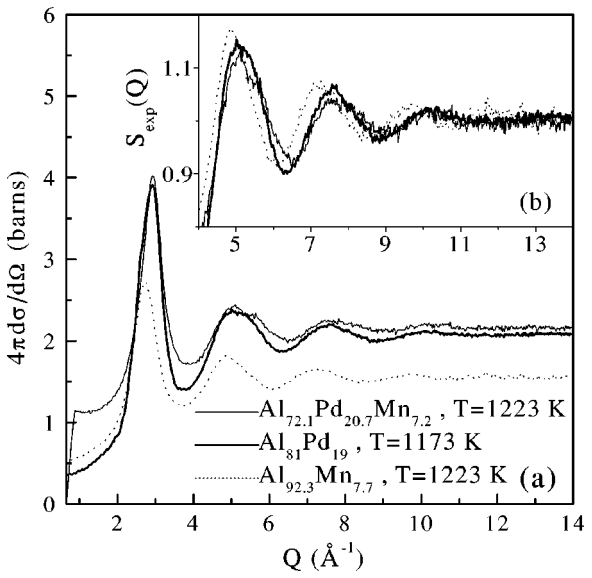

FIG. 3. Differential scattering cross section (a) and structure factors at large Q (b) of the $Al_{92.3}Mn_{7.7}$, $Al_{81}Pd_{19}$, and $Al_{72.1}Pd_{20.7}Mn_{7.2}$ (from Ref. 13) liquids.

of $Al_{72.1}Pd_{20.7}Mn_{7.2}$ measured in the same experimental conditions (from Ref. 13). At small-Q values, there are paramagnetic contributions in both $Al_{12}Mn$ and $Al_{72.1}Pd_{20.7}Mn_{7.2}$ alloys. The structure factors of these three liquids are shown in the inset [Fig. 3(b)] for large-Q values where the influence of local order is predominant (cf. Sec. IV). The oscillations of $Al_{81}Pd_{19}$ and $Al_{72.1}Pd_{20.7}Mn_{7.2}$ liquid structure factors are very similar, while, for $Al_{92.3}Mn_{7.7}$, the oscillations are shifted to smaller Q values. This suggests a different local order in $Al_{92.3}Mn_{7.7}$ on the one hand, and in $Al_{81}Pd_{19}$ and $Al_{72.1}Pd_{20.7}Mn_{7.2}$ liquids on the other hand.

III. PARTIAL STRUCTURE FACTORS AND PAIR DISTRIBUTION FUNCTIONS

Partial structure factors were determined in liquid $Al_{88.5}(Mn_xCr_{1-x})_{11.5}$ alloys using the formalism of both Faber and Ziman[25] and Bhatia and Thornton.[26] A subtraction of the paramagnetic scattering $d\sigma_{mag}/d\Omega(Q)$ was first applied in order to obtain $S_{expt}(Q)$. The procedure is given in the Appendix.

The Faber-Ziman formalism gives access to Al-Al, Al-M and M-M partial structure factors and related pair distribution functions $g(r)$. M is the average transition-metal atom Mn_xCr_{1-x}.

$$S_{FZ}(Q)=\frac{\langle b^2\rangle}{\langle b\rangle^2}S_{expt}(Q)-\frac{\sigma_{inc.M}}{4\pi\langle b\rangle^2}-\frac{\langle b^2\rangle-\langle b\rangle^2}{\langle b\rangle^2}, \quad (2)$$

$$S_{FZ}=\sum_{i,j=Al,M} W_{ij}S_{ij}(Q)=\sum_{i,j=Al,M}\frac{c_ic_j\overline{b_i}\,\overline{b_j}}{\langle b\rangle^2}S_{ij}(Q), \quad (3)$$

with $\langle b\rangle=\Sigma_{j=Al,M}c_j\overline{b_j}$ and $\langle b^2\rangle=\Sigma_{j=Al,M}c_j\overline{b_j^2}$. c_M and $\overline{b_M}=x\overline{b_{Mn}}+(1-x)\overline{b_{Cr}}$ are the average atomic concentration and coherent scattering length of M atoms, respectively. $\sigma_{inc.M}=4\pi c_M[(x\overline{b_{Mn}^2}+(1-x)\overline{b_{Cr}^2})-\overline{b_M^2}]$ is the incoherent scattering cross-section due to the mixture of Mn and Cr atoms.

TABLE II. W_{ij} and W_{NC} coefficients of the pair partial structure factors for each liquid $Al_{88.5}(Mn_xCr_{1-x})_{11.5}$ phase sample, using the definition of Faber and Ziman [Eq. (3)] and Bhatia and Thornton [Eq. (5)].

x	W_{TMTM}	W_{AlAl}	W_{AlTM}	W_{NN}	W_{NC}	W_{CC}
1	0.0267	1.3538	−0.3805	0.5675	−3.1059	0.4325
0.745	0.0056	1.1547	−0.1603	0.7394	−2.7592	0.2606
0.494	0.0000	1.0002	−0.0002	0.8848	−2.0014	0.1152
0.246	0.0042	0.8748	0.1210	0.9751	−0.9732	0.0249
0	0.0145	0.7734	0.2120	0.9997	0.1072	0.0003

The Bhatia-Thornton formalism describes the correlation between density (N) and concentration (C), yielding C-C, N-C, and N-N partial structure factors and pair distribution functions. In particular, the N-N partial functions correspond to a hypothetical liquid with the same structure as those studied, but whose atoms have the same coherent length. It allows one to probe the geometrical order only,

$$S_{BT}(Q)=S_{expt}(Q)-\frac{\sigma_{inc.M}}{4\pi\langle b^2\rangle}, \quad (4)$$

$$\begin{aligned}S_{BT}(Q)&=\sum_{N,C}W_{NC}S_{NC}(Q)\\&=\frac{\langle b\rangle^2}{\langle b^2\rangle}S_{NN}(Q)+\frac{2\Delta b\langle b\rangle}{\langle b^2\rangle}S_{NC}(Q)\\&\quad+\frac{c_{Al}c_M(\Delta b)^2}{\langle b^2\rangle}S_{CC}(Q),\end{aligned} \quad (5)$$

where $\Delta b=\overline{b_M}-\overline{b_{Al}}$.

The W_{ij} and W_{NC} coefficients of the partial functions, as defined in the general equations (3) and (5), are gathered in Table II. Because of uncertainties concerning the total structure factor measured on the $Al_{88.5}Mn_{11.5}$ sample, the partial functions were determined from four liquid $Al_{88.5}(Mn_xCr_{1-x})_{11.5}$ alloys ($x=0.745$–0). The partial structure factors and corresponding pair distribution functions, determined by Fourier transform (performed between 0.7 and 10 Å^{-1}) for both Bhatia-Thornton and Faber-Ziman formalisms, are represented in Fig. 4. As only three total structure factors are necessary to extract partial structure factors, a mathematical method for the treatment of overdimensioned systems was applied in order to obtain a better accuracy.[33] The W_{AlM} and W_{MM} coefficients, corresponding to the total structure factor of a liquid sample with $x=0.494$, being almost zero (Table II), this structure factor is expected to be almost identical to $S_{AlAl}(Q)$. This is actually the case. We also calculated the partial structure factors $S_{AlAl}(Q)$ and $S_{AlM}(Q)$ by using all possible combinations of three measured structure factors among the four previous ones. They remain identical within experimental accuracy, and are in agreement with those shown in Fig. 4. All these

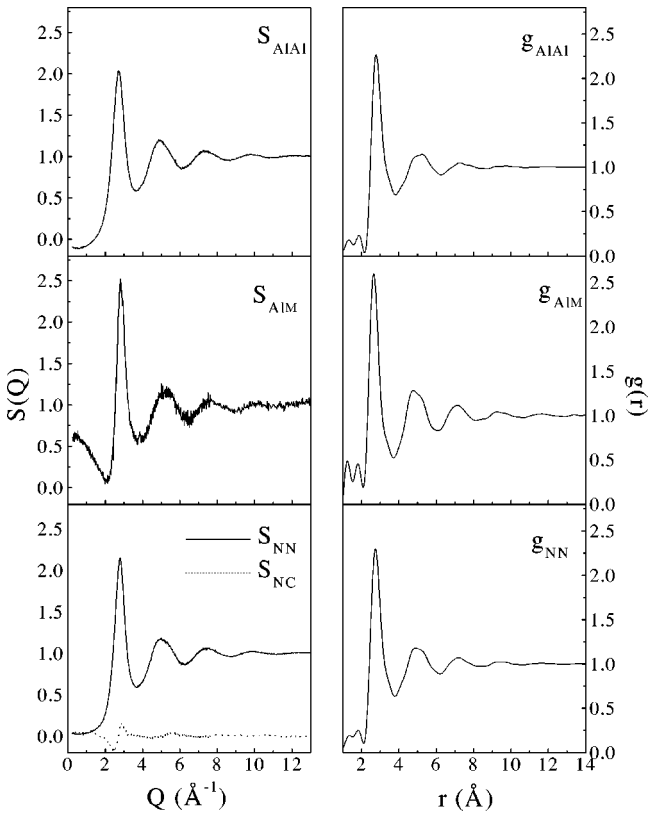

FIG. 4. Partial structure factors (left) and pair distribution functions (right) extracted from four $Al_{88.5}(Mn_xCr_{1-x})_{11.5}$ liquid spectra ($x=0.745$, 0.494, 0.246, and 0) at 1343 K in Faber-Ziman and Bhatia-Thornton formalisms.

analyses ascertain our initial hypothesis of a Mn/Cr isomorphous substitution. The *M*-*M* and *C*-*C* partial functions are not represented because of important inaccuracies resulting from the small proportion of *M* atoms in the liquid samples. Such inaccuracies were indeed predicted from an analysis of partial pair functions in the case of the μ phase compounds.[17]

The positions of the first peak of the g_{AlM} and g_{AlAl} partial pair distribution functions are at 2.65 and 2.78 Å, respectively. These distances are slightly higher than in the μ phase compounds. It can be pointed out that their ratio, equal to 1.048, is very close to that of a regular icosahedron of 12 Al surrounding a *M* atom ($\langle r_1\rangle/\langle r_0\rangle=1.0515$). From integral calculations of the related radial distribution functions [equal to $4\pi r^2\rho g(r)dr$, with ρ the number of atoms per unit volume density] between 2.08 and 3.64 Å, the pair coordination number corresponding to the first peak of g_{AlM}, g_{AlAl}, and g_{NN} (total coordination number involving all chemical species) were found to be equal to 10.5, and 10.6, and 11.9, respectively. They are very close to those existing in the μAl_4Mn structure. In this phase, 98.2% of Mn atoms are surrounded by icosahedra of either 11Al+1Mn or 10Al +2Mn. All these structural features are then in agreement with an icosahedral local order. In addition, let us point out that the first peak of g_{AlM} is narrower and higher in amplitude than this of g_{AlAl}; At larger *r* values, the oscillations of the Al-*M* pair distribution exhibit greater amplitudes than those of the Al-Al pair distribution. Thus, the Al-*M* correlations are stronger than the Al-Al ones, and Al-*M* local chemical order prevails in these liquids. Therefore, a strong Al-*M* order coupled to a favorable Al/*M* atomic size ratio effect could be at the origin of a strong icosahedral local order in both Al-*M* liquids and equilibrium solid phases.

IV. SIMULATION AT LARGE MOMENTUM TRANSFER

A. Method

The hypothesis of an icosahedral local order in Al-*M* liquid alloys can be investigated by simulations of the measured total structure factors at large-*Q* values. Let us recall that an analysis of the structure factor at large *Q* is possible under several conditions. The principle of the method, initially introduced to describe molecular solids,[34–36] was adapted and applied in a previous work to simulations of the structure factor of liquid Al-Pd-Mn alloys forming either quasicrystals or approximant phases.[13] Its application to liquid Al-Mn-Cr alloys implies that a cluster, with a lifetime longer than the time of interaction with neutrons ($t\geqslant 10^{-10}$ s), can be defined in the liquid, and that the atoms within the cluster are more rigidly bound together than to other atoms in the system (i.e., the clusters are only weakly coupled between them). The basic idea of the analysis is that, at increasing *Q* values, the Debye-Waller factor relative to the motion of the center of mass of the cluster is vanishing (diffusive motion characteristics of a liquid), while the Debye-Waller factor $\exp(-2W_{kl})$, due to the internal motions of the cluster and corresponding to the thermal changes ($\langle \delta r_{kl}^2\rangle$) of the distance r_{kl} between atoms *k* and *l* of a same cluster, remains finite. Thus at large *Q*, the structure factor essentially reflects the contribution of short intracluster pair distances. For a liquid containing rigidly bound clusters and neglecting intercluster contributions, the structure factor can be written as

$$S(Q)-1 = \frac{1}{N_{at}\langle b^2\rangle}\sum_{k,l=1(k\neq l)}^{N_{at}} \overline{b_k}\,\overline{b_l}\,\frac{\sin(Q\langle r_{kl}\rangle}{Q\langle r_{kl}\rangle}\exp(-2W_{kl}), \tag{6}$$

where N_{at} is the number of atoms within each cluster, and $\langle r_{kl}\rangle$ the average value of the distance between atoms *k* and *l* within the cluster. The adjustable parameters in Eq. (5), once the chemistry and geometry of the cluster are chosen, are the mean pair distances $\langle r_{kl}\rangle$ within the clusters and the associated mean distance variations $\langle \delta r_{kl}^2\rangle$ which enter the Debye-Waller factor expression: $\exp(-2Q^2\langle \delta r_{kl}^2\rangle/3)$. For instance, the geometry of the icosahedral cluster is characterized by four mean pair distances $\langle r_i\rangle$ related between them by $\langle r_1\rangle=1.0515\langle r_0\rangle$, $\langle r_2\rangle=1.7013\langle r_0\rangle$, and $\langle r_3\rangle=2\langle r_0\rangle$. The pair distance $\langle r_0\rangle$ occurs between the central atom and one atom of the icosahedral shell, and $\langle r_1\rangle$, $\langle r_2\rangle$, and $\langle r_3\rangle$ correspond to first-, second-, and third-neighbor atomic distances on the icosahedral shell, respectively. Note that in the *Q* range where the comparisons between experimental and

simulated structure factors are made ($4.5<Q<14$ Å^{-1}), the paramagnetic contributions are almost zero.

Using this large-Q simulation method, we first check the presence of icosahedral local order in $Al_{88.5}(Mn_xCr_{1-x})_{11.5}$ liquids on account of the results of a partial function analysis. Then, we present a study of the local order of other Al-based liquid alloys: an $Al_{92.3}Mn_{7.7}$ liquid, whose composition allows one to accommodate all Mn atoms in the center of Al icosahedra, and in which the partial functions were not extracted; an $Al_{80}Ni_{20}$ liquid, whose crystallization products do not present icosahedral local order; and an $Al_{81}Pd_{19}$ liquid, in order to understand the role of Pd atoms in the local order of ternary Al-Pd-Mn liquids.

B. Al-Mn-Cr liquids

Simulations of the structure factor of liquid $Al_{88.5}(Mn_xCr_{1-x})_{11.5}$ alloys were performed using the general results of a partial function analysis: the presence of icosahedral local order and the presence of strong chemical M-Al order. $(AlM)_{12}M$ icosahedral clusters were considered to be constituted of a central M atom of average scattering length $\overline{b}_M=x\overline{b}_{Mn}+(1-x)\overline{b}_{Cr}$ surrounded by 12 atoms of average scattering length $0.959\overline{b}_{Al}+0.041\overline{b}_M$ (i.e., chosen according to the residual liquid composition). In this model, all the atoms are embedded in icoshedra, but only 67% of the M atoms occupy the center of icosahedra. The $\langle r_0\rangle$ value and the mean thermal variations of the distances $\langle \delta r_i^2\rangle$ were left free in the simulation.

Simulations of the $Al_{88.5}(Mn_xCr_{1-x})_{11.5}$ liquids ($x=1$, 0.745, 0.494, 0.246, and 0) based on such icosahedra were found to be in good agreement with experimental structure factors for Q values larger than 6.5 Å^{-1} (Fig. 5). Departures from simulations and experimental results are systematically observed at Q values lower than 6.5 Å^{-1}, as inter-cluster contributions become non-negligible. The $\langle r_0\rangle$ and $\langle \delta r_i^2\rangle$ values entering into simulations are listed in Table III. Note that the optimized $\langle \delta r_i^2\rangle$ values increase with $\langle r_i\rangle$, and that the optimized pair distance $\langle r_0\rangle$ is slightly smaller than the position of the first peak of $g_{AlM}(r)$ as determined in Sec. III. This latter result will be discussed in Sec. V. The fitted parameters are the same for all $Al_{88.5}(Mn_xCr_{1-x})_{11.5}$ liquids within the experimental accuracy (± 0.01 Å for $\langle r_0\rangle$ and ± 0.003 Å^2 for $\langle \delta r_i^2\rangle$). Thus the evolution of the structure factor at large Q (shift of the oscillations towards larger Q as x decreases) is due to the contrast variation between Mn and Cr scattering lengths. Such an agreement between simulated and experimental structure factors for all liquids satisfies the assumption that the Mn/Cr substitution in the liquid state is isomorphic. Note that a simulation assuming no chemical order (i.e., the same value of the scattering length $0.885\overline{b}_{Al}+0.115\overline{b}_M$ for all atoms of the icosahedron) does not reproduce the shift of oscillations as a function of the Mn/Cr ratio variation. The origin of this shift is illustrated in Fig. 5, where the contributions of atomic pairs corresponding to the two shortest pair distances of the icosahedron (the contribution of the two largest pair distances is much smaller) are shown together with the simulated total structure factors of

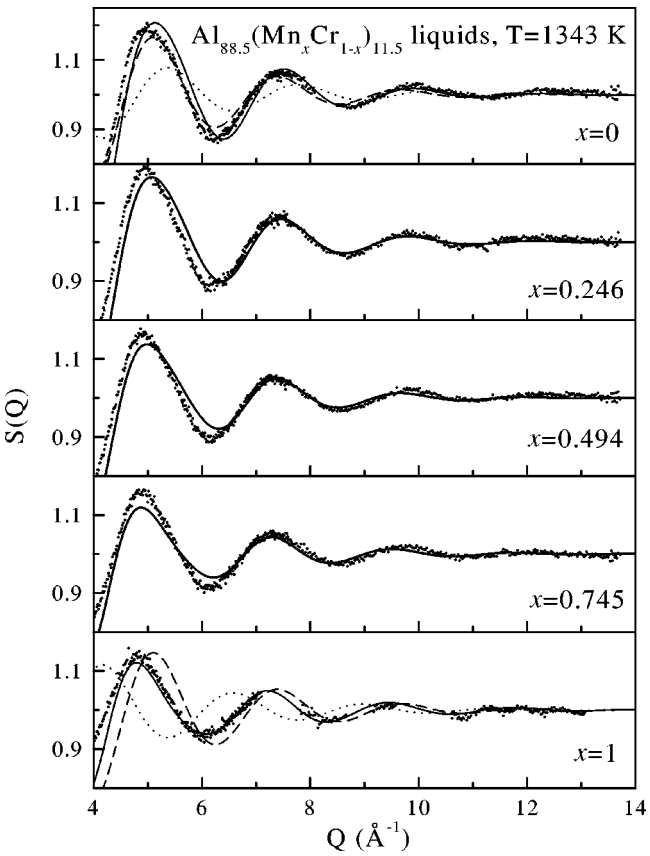

FIG. 5. Comparison for $Q\geqslant 4$ Å^{-1} of the measured structure factor of $Al_{88.5}(Mn_xCr_{1-x})_{11.5}$ liquids (dots) with calculated structure factors (solid lines) from a model of $(AlM)_{12}M$ icosahedra (see text). For the two binary liquids, the two shortest icosahedral pair distance ($\langle r_0\rangle$ and $\langle r_1\rangle$) contributions to the simulations are displayed by dotted and dashed lines, respectively. Parameters of the simulation are given in Table III.

$Al_{88.5}Cr_{11.5}$ and $Al_{88.5}Mn_{11.5}$ liquids. When substituting Mn with Cr, the $S(Q)$ corresponding to the first pair distance $\langle r_0\rangle$ contribution is shifted toward larger Q values, while the $S(Q)$ corresponding to the second pair distance $\langle r_1\rangle$ contribution is almost unchanged. Let us note that the presence of two different short pair distances within the icosahedral cluster can be related to the asymmetry of the second oscillation at around 5.5 Å^{-1} for all $Al_{88.5}(Mn_xCr_{1-x})_{11.5}$ liquid structure factors. In particular, for an $Al_{88.5}Cr_{11.5}$ liquid with almost the same coherent length for all atoms, the first pair distance contribution produces a shoulder on the right side of the second oscillation. This shoulder is often interpreted as the signature of an icosahedral local order.[15,37,38]

C. Al-Mn liquid

As $Al_{92.3}Mn_{7.7}$ and $Al_{88.5}Mn_{11.5}$ liquids both present a primary crystallization of μ phase, a close local order can be expected. A simulation was performed with all Mn atoms in the centers of Al icosahedra as allowed by the liquid stoichiometry. An excellent agreement between experiment and simulation is found in a Q range (from 4 to 14 Å^{-1}) larger

TABLE III. Parameters of the simulation, based on icosahedral clusters, for different liquid alloys. The distances are in Å, and the mean distance variation in Å ^{2}. The typical error is ± 0.01 Å on the first distance $\langle r_0 \rangle$ and ± 0.003 Å^2 on the mean distance variation $\langle \delta r_j^2 \rangle$.

	$\langle r_0 \rangle$	$\langle r_1 \rangle$	$\langle r_2 \rangle$	$\langle r_3 \rangle$	$\langle \delta r_0^2 \rangle$	$\langle \delta r_1^2 \rangle$	$\langle \delta r_2^2 \rangle$	$\langle \delta r_3^2 \rangle$
$Al_{88.5}(Mn_xCr_{1-x})_{11.5}$	2.61	2.74	4.43	5.21	0.03	0.04	0.105	0.135
$Al_{12}Mn$	2.59	2.72	4.40	5.17	0.03	0.033	0.105	0.135
$Al_{81}Pd_{19}$	2.59	2.72	4.40	5.17	0.037	0.045	0.105	0.135
$Al_{72.1}Pd_{20.7}Mn_{7.2}$	2.59	2.72	4.40	5.17	0.03	0.039	0.105	0.135
$Al_{80}(Mn_xCrFe_{1-x})_{20}$	2.55	2.68	4.34	5.10	0.033	0.043	0.105	0.135
$Al_{80}Ni_{20}$	2.52	2.65	4.29	5.04	0.039	0.052	0.105	0.135

than in the case of $Al_{88.5}(Mn_xCr_{1-x})_{11.5}$ liquids (Fig. 6). The first distance value $\langle r_0 \rangle$ is 2.59 Å (Table III), i.e., close to the values used for the $Al_{88.5}(Mn_xCr_{1-x})_{11.5}$ simulation.

In order to test the relevance of such simulations, we also calculated the structure factor of another compact cluster containing 13 atoms, but with another geometry: an Al cuboctahedron centered on a Mn atom for which $\langle r_1 \rangle = \langle r_0 \rangle$, $\langle r_2 \rangle = \sqrt{2}\langle r_0 \rangle$, $\langle r_3 \rangle = \sqrt{3}\langle r_0 \rangle$, and $\langle r_4 \rangle = 2\langle r_0 \rangle$. In this case, for Q values lower than 6 Å^{-1}, the simulation starts to depart from the experiment and is clearly less good than the simulation based on icosahedral clusters (Fig. 6). The optimized parameters for this simulation are $\langle r_0 \rangle = \langle r_1 \rangle = 2.75$ Å (± 0.01 Å) and $\langle \delta r_i^2 \rangle = 0.015$, 0.015, 0.075, 0.09, and 0.105 Å^2 (± 0.003 Å^2) for $i = 0$–4, respectively.

D. Al-Ni liquid

Finally, we checked that a simulation based on a liquid model of icosahedral clusters does not describe a liquid Al-Ni alloy whose solidification into intermetallic phases does not correspond to the formation of quasicrystalline or approximant phases. For this purpose, the simulation method was applied to the partial structure factors $S_{NN}(Q)$ experimentally determined by Maret *et al.*[11] on $Al_{80}[Mn_x(Cr_{0.5}Fe_{0.5})_{1-x}]_{20}$ and $Al_{80}Ni_{20}$ liquids with the same M content. Let us recall that the $S_{NN}(Q)$ partial structure factor in the Bhatia-Thornton formalism allows one to consider a geometrical order but not a chemical order. In Fig. 7, the $S_{NN}(Q)$ partial structure factor, obtained by Maret *et al.* from isotopic Ni substitution into $Al_{80}Ni_{20}$ liquids, is drawn with the corresponding simulation. It is compared to simulations of the experimental $S_{NN}(Q)$ structure factor of the liquids $Al_{80}[Mn_x(Cr_{0.5}Fe_{0.5})_{1-x}]_{20}$ (see the work of Maret *et al.*[11]) and of the liquids $Al_{88.5}(Mn_xCr_{1-x})_{11.5}$ (present work). For each case, the parameters of the simulation, based on icosahedral clusters, were adjusted so that the last calculated oscillation around 10–11 Å^{-1} is superimposed on the measured one (values in Table III). For both

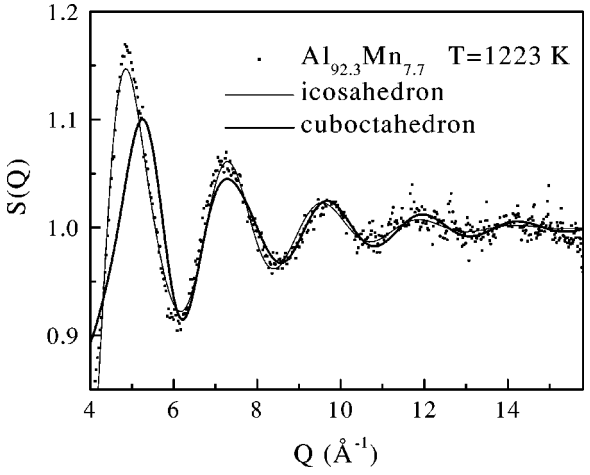

FIG. 6. Simulation of the $Al_{92.3}Mn_{7.7}$ structure factor based on an $Al_{12}Mn$ icosahedron (thin line) and an $Al_{12}Mn$ cuboctahedron (thick line). Parameters of the simulations are given in Table III and in the text.

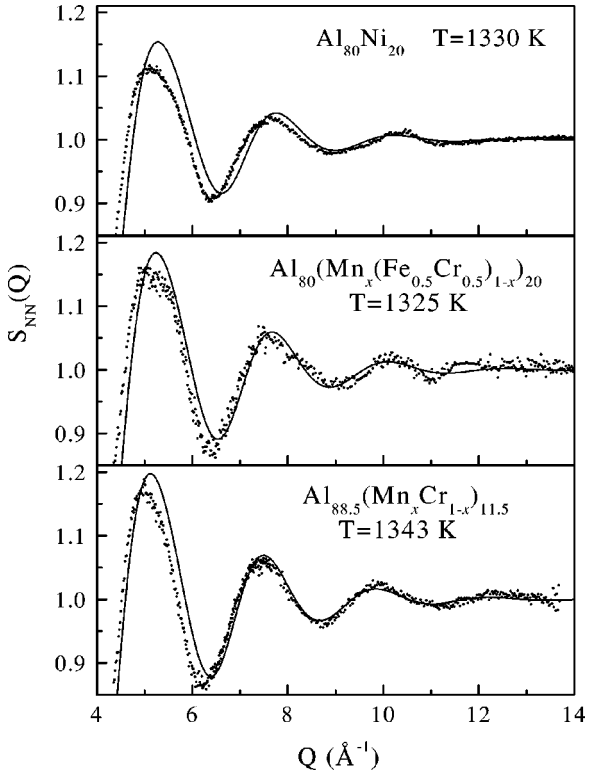

FIG. 7. Comparison of partial S_{NN} structure factors for $Al_{80}Ni_{20}$ (Ref. 11), $Al_{80}(Mn_x(Cr_{0.5}Fe_{0.5})_{1-x})_{20}$ (Ref. 11), and $Al_{88.5}(Mn_xCr_{1-x})_{11.5}$ liquids (dots) with calculated structure factors assuming that all atoms are embedded in icosahedra (solid lines). Parameters of the simulations are given in Table III.

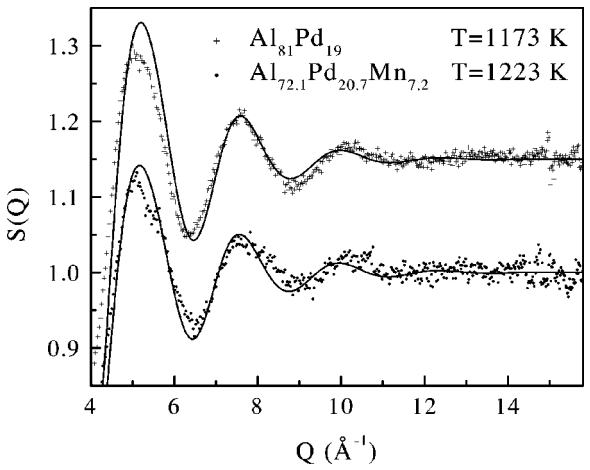

FIG. 8. Comparison of experimental structure factors for $Al_{81}Pd_{19}$ and $Al_{72.1}Pd_{20.7}Mn_{7.2}$ liquids with simulations based on $(AlPd)_{12}Pd$ and $(AlPdMn)_{12}(PdMn)$ icosahedra, respectively (see the text). Parameters of the simulations are given in Table III.

$Al_{80}[Mn_x(Cr_{0.5}Fe_{0.5})_{1-x}]_{20}$ and $Al_{88.5}(Mn_xCr_{1-x})_{11.5}$ liquids, the simulation reproduces the $S_{NN}(Q)$ function for Q values larger than 6.5 $Å^{-1}$ confirming the presence of icosahedral local order in Al-Mn-Cr(-Fe) liquids. Conversely, any other oscillations than the one chosen as reference could not be simulated in the case of the liquid $Al_{80}Ni_{20}$ alloy. This result confirms the conclusion of an absence of a local icosahedral order in this liquid $Al_{80}Ni_{20}$ alloy, obtained by Maret *et al.*[11] from an analysis based on molecular dynamics.

E. Al-Pd and Al-Pd-Mn liquids

In a previous work,[13] we performed simulations at large Q on the structure factor of an $Al_{72.1}Pd_{20.7}Mn_{7.2}$ liquid. In this case, the local order was analyzed by Al or AlPd icosahedra centered on Mn atoms with an $\langle r_0 \rangle$ distance of 2.44 Å. As it was difficult to understand why similar Mn-centered clusters would have different sizes in $Al_{92.3}Mn_{7.7}$ ($\langle r_0 \rangle = 2.6$ Å) and $Al_{72.1}Pd_{20.7}Mn_{7.2}$ liquids with similar Mn contents, further analyses were required.

We first tried to simulate the binary liquid $Al_{81}Pd_{19}$, whose large-Q oscillations are close to the $Al_{72.1}Pd_{20.7}Mn_{7.2}$ ones (as shown in Sec. II). For this liquid, a simulation based on $(AlPd)_{12}Pd$ icosahedra, constituted by a central Pd atom surrounded by 12 atoms of an average scattering length $0.877\overline{b}_{Al} + 0.123\overline{b}_{Pd}$, yields a reasonable agreement (Fig. 8). Note that Al icosahedra centered on Pd atoms are actually found in the o-Al_3Pd solid phase.[27] The first pair distance within this icosahedron, $\langle r_0 \rangle = 2.59$ Å, is found to be identical to that of the icosahedron used to describe the $Al_{92.3}Mn_{7.7}$ structure factor (cf. Table III for the other parameters).

Hence, to account for the $Al_{72.1}Pd_{20.7}Mn_{7.2}$ structure factor, a simulation based on a $(AlPdMn)_{12}(PdMn)$ icosahedron, centered on a mixture of Pd and Mn atoms ($0.742\overline{b}_{Pd} + 0.258\overline{b}_{Mn}$ on account of the alloy Pd/Mn stoechiometry), was made (Fig. 8). The outer icosahedral shell composition was chosen such that all atoms are embedded in icosahedra. Thus it is constituted by the remaining Al, Pd, and Mn atoms of average scattering length $0.781\overline{b}_{Al} + 0.162\overline{b}_{Pd} + 0.057b_{Mn}$. Note that this average scattering length is almost equal to that of Al; a simulation with a pure Al icosahedral shell is also therefore a possible solution. The first pair distance is equal to 2.59 Å, in agreement with the first distance of the icosahedra describing both $Al_{92.3}Mn_{7.7}$ and $Al_{81}Pd_{19}$ binary alloys. Let us note that the evolution of simulated structure factors from $Al_{81}Pd_{19}$ to $Al_{72.1}Pd_{20.7}Mn_{7.2}$, i.e., a decrease of the amplitude of the oscillations for Q values lower than 8 $Å^{-1}$, follows that of the experimental structure factors. Therefore, to describe the local order of Al-Pd-Mn liquids, Pd and Mn atoms have to be considered in the center of icosahedra.

V. DISCUSSION

From an analysis of partial functions and from simulations at large Q of measured structure factors, we have shown that the icosahedral local order found in $Al_{88.5}(Mn_xCr_{1-x})_{11.5}$ liquid alloys is driven by a strong chemical order between Al and transition-metal atoms: M atoms are at the centers of icosahedral clusters mainly constituted of Al atoms. Those clusters are similar to those found in the solid μ phase, and in most of the intermetallic phases on the Al-rich side of the Al-Mn, Al-Mn-Cr and Al-Cr phase diagrams (for example, $Al_{12}Mn$, $\lambda Al_{4.5}Mn$, $\phi Al_{10}Mn_3$, $Al_{11}Mn_4$, and $\theta Al_{45}Cr_7$). The relevance of the method of simulation at large Q is further validated by the disagreement of icosahedral-cluster-based simulations with the measured structure factor of a liquid $Al_{80}Ni_{20}$ alloy, which does not form icosahedral phases. This simulation method, applied to other Al-M liquids with different M content, $Al_{92.3}Mn_{7.7}$ and $Al_{80}[Mn_x(Cr_{0.5}Fe_{0.5})_{1-x}]_{20}$, shows that their local order can also be described by M-centered icosahedra. Therefore, Mn and Cr atoms (and also Fe from Ref. 8) appear to have a particular role in Al-based liquid alloys forming quasicrystals.

If the stoichiometry of the $Al_{92.3}Mn_{7.7}$ liquid allows one to accommodate all M atoms in the center of Al icosahedra, this is not the case for higher M content. For instance, the proportion of transition atoms located at the center of icosahedral clusters is only of 67% for the simulation of $Al_{88.5}(Mn_xCr_{1-x})_{11.5}$ liquids presented in Sec. IV B. If a M-Al chemical order prevails in the liquid state, a maximum number of M atoms would be expected to be surrounded by an icosahedron, mainly constituted of Al. In order to increase the proportion of transition atoms at the center of icosahedral clusters, one might either consider that clusters are linked between them as in the μ phase,[22] or that the atomic occupancy factors on icosahedral shell sites are less than 100%. Both hypotheses lead to simulations in good agreement with the experimental structure factors. The knowledge of the M-M pair distribution function, which could not be determined in the present work, would allow one to choose between both hypothesis.

Let us point out that in these liquids, due to atomic mo-

tions, the geometrical arrangement of atoms cannot be strictly icosahedral. The icosahedron, which is the most compact and symmetric way of packing 13 atoms, could be the ideal limit toward which the local structure of these Al-*M* liquids tends. The existence of a distribution of local environments can be inferred from the asymmetrical shape of the first peak of the $g_{AlM}(r)$ distribution function of $Al_{88.5}(Mn_xCr_{1-x})_{11.5}$ liquids (Fig. 4). This has to be compared to the $g_{AlM}(r)$ distribution function of the μ-phase compounds,[17] whose first peak is narrower and more symmetric with a maximum value at 2.59 Å. This value is very close to the $\langle r_0 \rangle$ value (2.61 Å) yielded by the large-*Q* simulation of $Al_{88.5}(Mn_xCr_{1-x})_{11.5}$ liquids. The difference between $\langle r_0 \rangle$ and the maximum of the $g_{AlM}(r)$ first peak (2.65 Å) in the $Al_{88.5}(Mn_xCr_{1-x})_{11.5}$ liquid may then be explained. Let us assume that the more rigid atomic pairs are those embedded in clusters tending to perfect icosahedra like those of the μ phases corresponding to the shortest pair distances. Then the simulation at large *Q*, which is mainly sensitive to rigid pairs, is optimized for a $\langle r_0 \rangle$ distance smaller than the maximum of the first peak of the $g_{AlM}(r)$ which is an average distribution of all *M*-Al atomic pairs. The proportion of atoms embedded in perfect icosahedra was determined by Maret *et al.*[11] through a molecular dynamics study of $Al_{80}[Mn_x(Cr_{0.5}Fe_{0.5})_{1-x}]_{20}$ liquids with a reversed Monte Carlo method using the pair potentials extracted from the experimental structure factors. These authors analyzed the structure in terms of Voronoï polyhedra, and found that only 22% of the atoms are embedded in perfect icosahedra. This is not in contradiction with the conclusions deduced from large-*Q* simulations, which take into account deformed icosahedral clusters owing to the Debye-Waller factor.

One may wonder what kind of local order occurs in a ternary $Al_{72.1}Pd_{20.7}Mn_{7.2}$ liquid. This liquid gives rise to stable icosahedral phases, whereas the icosahedral phases in the Al-Mn system are metastable. From comparison of the large-*Q* part of the structure factors, the local order appears to be different between $Al_{72.1}Pd_{20.7}Mn_{7.2}$ and $Al_{92.3}Mn_{7.7}$ liquids although they have the same Mn content. To study the role of Pd atoms, we performed large-*Q* simulations on the structure factor of a binary $Al_{81}Pd_{19}$ liquid alloy. As results, the simulation based on icosahedra centered on Pd atoms agrees with the measured structure factor. Then a large-*Q* simulation of the structure factor of $Al_{72.1}Pd_{20.7}Mn_{7.2}$ confirms that both Pd and Mn atoms are preferentially surrounded by Al atoms on an icosahedral shell. Therefore, in this Al-Pd-Mn alloy, the Pd atoms also play an important role in the liquid structure which is probably linked to the higher stability of the corresponding solid phases.

In summary, we have shown that a combination of different structural analyses—partial pair distribution function determination and a simulation of the structure factors at large *Q* values—allows one to obtain information on the local order of Al-*M* liquids. In Al-based liquids forming icosahedral or approximant phases as primary crystallizations, the local order can be described by icosahedra centered on *M* atoms, similar to those found in the equilibrium solid phases. From the resemblance of the solid and liquid local orders, a low solid-liquid interfacial energy, implying a reduction of undercooling phenomena, would then be expected. This is confirmed by temperature-time profiles recorded during undercooling experiments performed on various melts.[1] Actually, a deep undercooling was observed for melts forming crystalline phases, whereas reduced undercoolings were achieved for melts forming quasicrystalline phases.

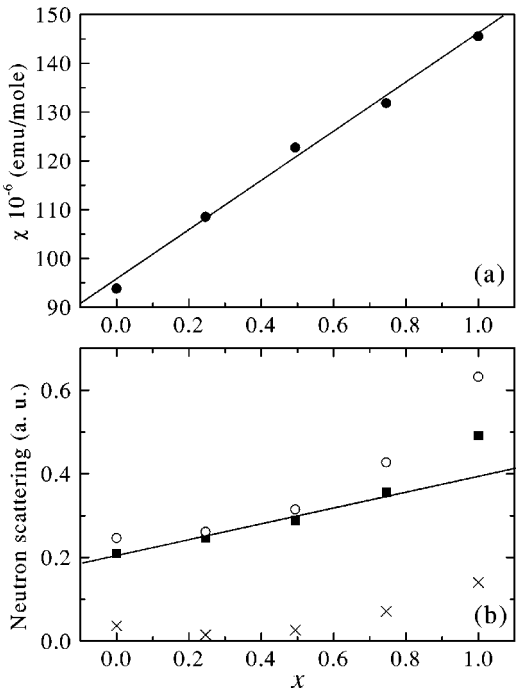

FIG. 9. Evolution, as a function of *x* for the different $Al_{88.5}(Mn_xCr_{1-x})_{11.5}$ liquid alloys at 1343 K, of (a) the magnetic susceptibility and (b) the differential scattering cross section corrected from incoherent scattering (σ_i and $\sigma_{inc.TM}$) at 0.7 $Å^{-1}$ (open circles), the calculated $4\pi\langle b^2\rangle S_{BT}(0)$ (crosses), and the difference between the two (black squares).

ACKNOWLEDGMENTS

We would like to thank H. Fischer and P. Palleau for their assistance during the neutron experiments on D4B, H. Klein for his participation to the neutron experiment on D4B, M. Maret for kindly sending us her experimental data on $Al_{80}Ni_{20}$ and $Al_{80}[Mn_x(CrFe)_{1-x}]_{20}$ alloys, and J. Blétry for fruitful discussions.

APPENDIX: PARAMAGNETIC SCATTERING CONTRIBUTION

The magnetic scattering has to be subtracted from the differential scattering cross sections measured on liquid $Al_{88.5}(Mn_xCr_{1-x})_{11.5}$ samples before determining partial functions. The existence of a paramagnetic scattering produced by *M* atoms in these liquids is confirmed by susceptibility measurements. The susceptibility of the solid phases is very small. A strong increase occurs upon melting, resulting from a large fraction of magnetic *M* atoms in the liquid phase.[23] As shown in Fig. 9(a), the susceptibility increases linearly with the Mn/Cr ratio, since Mn atoms bear a higher

magnetic moment than Cr atoms.

The measured signal at small Q is the sum of a paramagnetic scattering and of nuclear scattering contributions. According to Eqs. (1) and (4), the magnetic contribution at $Q \rightarrow 0$ can be deduced by subtracting both $4\pi\langle b^2\rangle S_{BT}(Q \rightarrow 0)$ and incoherent scattering values (σ_i and $\sigma_{inc.M}$) from the measured differential scattering cross section.

The expression of neutron paramagnetic scattering for noninteracting magnetic atoms can be written as

$$\frac{4\pi d\sigma_{mag}}{d\Omega}(Q) = \frac{8\pi}{3} c_M r_0^2 F^2(Q) S(S+1), \qquad \text{(A1)}$$

where $r_0 = -0.54 \times 10^{-12}$ cm, S is the spin quantum number of M atoms, c_M their atomic concentration, and $F(Q)$ their magnetic form factor [with $F(0)=1$]. Note that, when two kinds of M atoms are present, the quantity $c_M F^2(Q) S(S+1)$ should be replaced by the sum of their contributions.

The limit at $Q=0$ of the Bhatia-Thornton structure factor is given by[8]

$$4\pi\langle b^2\rangle S_{BT}(0) = 4\pi\langle b\rangle^2 \rho k_B T \chi_T + 4\pi(\langle b\rangle\delta - \Delta b)^2 c_M c_{Al} S_{CC}(0) \qquad \text{(A2)}$$

where χ_T is the isothermal compressibility, δ a dilatation factor defined by:

$$\delta = \frac{1}{V}\left(\frac{\partial V}{\partial c_M}\right)_{T,P} \qquad \text{(A3)}$$

and $S_{CC}(0)$ is related to the Gibbs energy G and Avogadro number N_a by

$$S_{CC}(0) = N_a k_B T / \left(c_M c_{Al} \left(\frac{d^2 G}{d c_M^2} \right)_{T,P} \right). \qquad \text{(A4)}$$

For each liquid alloy sample, the $S_{BT}(0)$ value was estimated on account of $S_{CC}(0)$ and δ values taken equal to 0.5 and -0.6, respectively.[8] The isothermal compressibility, defined as

$$\chi_T = \frac{C_p}{C_v \rho u^2}, \qquad \text{(A5)}$$

is calculated using the ratio of specific heats at constant pressure and at constant volume[39] equal to 1.15, a sound velocity[40] $u = 4400$ ms^{-1} and a density[41] $\rho = 0.055$ at.%Å^{-3} measured for a $Al_{90}Mn_{10}$ liquid above T_L.

The calculated values for $4\pi\langle b^2\rangle S_{BT}(0)$, and the measured differential scattering cross section corrected from incoherent scattering, are shown in Fig. 9(b). The difference, which is expected to correspond to paramagnetic scattering with the assumption that $S_{BT}(Q)$ is constant from $Q=0$ to 0.7 Å^{-1}, lies on a straight line for $x=0$ to 0.745 like the susceptibility [cf. Fig. 9(b)]. For $x=1$, the resulting value departs from this straight line, probably because the first peak of the structure factor also contributes at $Q=0.7$ Å^{-1}. The paramagnetic scattering was evaluated in this case by extrapolating the straight line to its value at $x=1$. According to Eq. (A1) and using the theoretical magnetic form factor[42,43] of Mn^{2+} (Mn and Cr magnetic form factors are very close), we determined a paramagnetic contribution which extends up to about 6 Å^{-1} and subtracted it from the total structure factors of the $Al_{88.5}(Mn_xCr_{1-x})_{11.5}$ liquids.

*Present address: DRFMC/SPSM-MDM, CEA-Grenoble, 17 rue des martyrs, 38402 Grenoble Cedex, France.

[1] D. Holland-Moritz, Int. J. Non-Equilib. Process. **11**, 169 (1998).
[2] F. C. Franck, Proc. R. Soc. London, Ser. A **215**, 43 (1962).
[3] P. J. Steinhardt, D. R. Nelson, and M. Ronchetti, Phys. Rev. B **28**, 784 (1983).
[4] H. Jonsson and H. C. Andersen, Phys. Rev. Lett. **60**, 2295 (1988).
[5] D. Shechtman, I. Blech, D. Gratias, and J. W. Cahn, Phys. Rev. Lett. **53**, 1951 (1984).
[6] D. Shechtman and I. Blech, Metall. Trans. A **16**, 332 (1985).
[7] P. W. Stephens and A. I. Goldman, Phys. Rev. Lett. **56**, 1168 (1986).
[8] M. Maret, A. Pasturel, C. Senillou, J. M. Dubois, and P. Chieux, J. Phys. (France) **50**, 295 (1989).
[9] M. Maret, P. Chieux, J. M. Dubois, and A. Pasturel, J. Phys.: Condens. Matter **3**, 2801 (1991).
[10] M. Maret, J. M. Dubois, and P. Chieux, J. Non-Cryst. Solids **156-158**, 918 (1993).
[11] M. Maret, F. Lançon, and L. Billard, Physica B **180-181**, 854 (1992); J. Phys. (France) **3**, 1873 (1993).
[12] F. Hippert, M. Audier, H. Klein, R. Bellissent, and D. Boursier, Phys. Rev. Lett. **76**, 54 (1996).
[13] V. Simonet, F. Hippert, H. Klein, M. Audier, R. Bellissent, H. Fischer, A. P. Murani, and D. Boursier, Phys. Rev. B **58**, 6273 (1998).
[14] M. Audier, M. Durand-Charre, and M. de Boissieu, Philos. Mag. B **68**, 607 (1983).
[15] S. Sachdev and D. R. Nelson, Phys. Rev. Lett. **53**, 1947 (1984); Phys. Rev. B **32**, 4592 (1985).
[16] S. Sachdev and D. R. Nelson successfully compared their description of the structure factor based on a Landau description of short-range icosahedral order to the experimental structure factor of amorphous Co. Moreover, recent evidence for the formation of clusters with fivefold symmetry in liquid lead at the interface to solid Si, measured by the scattering of evanescent x rays, was obtained by H. Reichert, O. Klein, H. Dosch, M. Denk, V. Honkimaeki, T. Lippmann, and G. Reiter, Nature (London) **408**, 839 (2000).
[17] V. Simonet, F. Hippert, M. Audier, and R. Bellissent, Physica B (to be published).
[18] T. Schenk, M. Durand-Charre, and M. Audier, J. Alloys Compd. **281**, 249 (1998).
[19] T. Schenk, H. Klein, M. Audier, V. Simonet, F. Hippert, J. Rodriguez-Carvajal, and R. Bellissent, Philos. Mag. Lett. **76**, 189 (1997).
[20] $b_{Mn} = -3.723$ and $b_{Cr} = 3.635$ from Neutron News **3**, 29 (1992).

[21] P. Guyot and M. Audier, Philos. Mag. B **52**, L15 (1985).
[22] C. Brink-Shoemaker, D. A. Keszler, and D. P. Shoemaker, Acta Crystallogr., Sect. B: Struct. Sci. **45**, 13 (1989).
[23] V. Simonet, F. Hippert, M. Audier, and R. Bellissent, J. Non-Cryst. Solids **250-252**, 824 (1999).
[24] V. Simonet, F. Hippert, M. Audier, and R. Bellissent, Mater. Sci. Eng. **294-296**, 116 (2000).
[25] T. E. Faber and J. M. Ziman, Philos. Mag. **11**, 153 (1965).
[26] A. B. Bhatia and D. E. Thornton, Phys. Rev. B **2**, 3004 (1970).
[27] Y. Matsuo and K. Hiraga, Philos. Mag. Lett. **70**, 155 (1994).
[28] M. Boudard, H. Klein, M. de Boissieu, M. Audier, and H. Vincent, Philos. Mag. A **74**, 939 (1996).
[29] H. H. Paalman and C. J. Pings, J. Appl. Phys. **33**, 2635 (1962).
[30] G. Placzek, Phys. Rev. **86**, 377 (1952).
[31] J. L. Yarnell, M. J. Katz, R. G. Wenzel, and S. H. Koenig, Phys. Rev. A **7**, 2130 (1973).
[32] I. A. Blech and B. L. Averbach, Phys. Rev. **137**, A1113 (1965).
[33] J. P. Simon, O. Lyon, and D. de Fontaine, J. Appl. Crystallogr. **18**, 230 (1985).
[34] G. Dolling, B. M. Powell, and V. F. Sears, Mol. Phys. **6**, 37 (1979).
[35] P. Damay, F. Leclercq, and P. Chieux, Phys. Rev. B **41**, 9676 (1990).
[36] F. Leclercq, P. Damay, M. Foukani, P. Chieux, M. C. Bellissent-Funel, A. Rassat, and C. Fabre, Phys. Rev. B **48**, 2748 (1993).
[37] J.-F. Sadoc, J. Dixmier, and A. Guinier, J. Non-Cryst. Solids **12**, 46 (1973).
[38] P. Andonov and P. Chieux, J. Non-Cryst. Solids **93**, 331 (1987).
[39] O. J. Kleppa, J. Chem. Phys. **18**, 1331 (1950).
[40] V. I. Stremousov and V. V. Tekuchev, Russ. J. Phys. Chem. **51**, 206 (1977).
[41] *Handbook of Chemistry and Physics* (CRC Press, Boca Raton, FL, 1981).
[42] R. E. Watson and A. J. Freeman, Acta Crystallogr. **14**, 27 (1961).
[43] P. J. Brown, in *International Tables for Crystallography*, edited by A. J. C. Wilson (Kluwer, Dordrecht, 1992).